Autori:

Matijasevic,L., Petrovic,P.

Naziv rada:

Underactuated Finger Design for Flexible Grasping in Robotic Assembly

Konferencija:

6th International Conference on Electrical, Electronic and Computing Engineering, IcETRAN 2019, Silver Lake, Serbia, June 03 – 06, 2019

Zbornik radova:

Proceedings of Papers, ISBN 978-86-7466-785-9, pp.730-735

PROCEEDINGS OF PAPERS

Zbornik radova

(Ic)ETRAN 2019

6th International Conference on Electrical, Electronic and Computing Engineering

in conjunction with

ETRAN

63rd National Conference on Electrical, Electronic and Computing Engineering

PROCEEDINGS OF PAPERS

Zbornik radova

(Ic)ETRAN 2019

6th International Conference on Electrical, Electronic and Computing Engineering

in conjunction with

ETRAN

63rd National Conference on Electrical, Electronic and Computing Engineering

Proceedings of Papers – 6th International Conference on Electrical, Electronic and Computing Engineering, IcETRAN 2019, Silver Lake, Serbia, June 03 – 06, 2019

Zbornik radova - 63. Konferencija za elektroniku, telekomunikacije, računarstvo, automatiku i nuklearnu tehniku, Srebrno jezero, 03 – 06. juna, 2019. godine

Main Editor / Glavni urednik
Dejan Popović

Editors / Urednici
Slobodan Vukosavić, Boris Lončar

Published by / **ETRAN Society, Belgrade, Academic Mind, Belgrade**
Izdavači / **Društvo za ETRAN, Beograd i Akademska misao, Beograd**

Production / Izrada
Academic Mind, Belgrade / Akademska misao, Beograd

Place and year of publication / Mesto i godina izdanja
Belgrade, 2019. / Beograd, 2019.

Circulation / Tiraž
200 primeraka / 200 copies

ISBN 978-86-7466-785-9

www.etran.rs

Nuclear engineering and technology / Nuklearna tehnika

Robotics and Flexible Automation / Robotika i fleksibilna automatizacija

Underactuated Finger Design for Flexible Grasping in Robotic Assembly

Lazar Matijašević, *PhD Student*, Petar B. Petrović, *Full Professor*

Abstract—**At present-day manufacturing and assembly lines, fairly simple mechanism grippers are used. On the other hand, growing demand for customized products that are mass produced, require flexible, multipurpose grippers that are capable of grasping complex objects of different sizes and shapes. In order for robotic hand to be industry acceptable it needs to be robust, easy to control and most importantly it needs to be affordable price-wise. With that in mind concept of multifingered underactuated robotic hand appears as a good candidate to be optimal, general purpose solution. Underactuation as a concept allows robotic hands to grip arbitrary shaped objects without the need for complex control and sensory systems. Also, with less actuators than degrees of freedom multifingered underactuated robotic hand is more affordable and from robot arm carrying capacity standpoint, actuators with less weight allows robotic systems to move faster or to carry heavier loads. For this research linkage driven underactuated mechanisms are chosen because of their rigidity and that trait makes control system more reliable and easier to make thus making whole robotic system more robust and reliable. This paper presents some aspects of design and grasping force analysis of three degrees of freedom (3-DoF) underactuated robotic finger with linkage driven mechanism for CMSysLab Robotic Hand.**

Index Terms—**Robotic Assembly, Robotic Hand, Design; Underactuation;**

I. Introduction

In industry setting, grasping of various objects in a well-structured or unstructured environment present complex tasks that are still performed by human operators even if environment is dangerous. The new production paradigm of mass customization and extensive needs for application of robotic technology in domain of Small and Medium Enterprises (SME), imposes demands for highly flexible, multipurpose gripers that are capable of precise and reliable grasping complex objects of different sizes and shapes, including in hand manipulation. In order to accommodate demands of mass customization and market push for ubiquitous use of robotic technology in SME operations, both robotic arms and robotic hands that approach performances of humans in terms of dexterity and adaptation capabilities must be developed, [1].

Robotic hands that can, to some degree, mimic human hand capabilities are using principle of complete actuation. One example of fully-actuated robotic hand is Shadow Dexterous Hand [2]. These fully-actuated robotic hands have some disadvantages like: space needed to put all actuators in, increased weight of such hand, complexity of control system needed to operate properly and biggest one, from application point of view, is high price of these hands.

On the other hand, prototypes are made that involve a smaller number of actuators than degrees of freedom. This approach, called underactuation is implemented through the use of passive elements like mechanical limits and springs leading to a mechanical adaptation of the finger to the shape of the object to be grasped.

In case of robotic grasping, underactuation allows the robotic hand to adjust itself to a wide range of shapes, including irregularly shaped objects, without the need for complex control strategies, sensory systems for feedback and replaceable mechanical parts. These underactuated robotic hand systems don't need complex control systems to operate, also have smaller mass and on top of that they are less expensive than fully actuated robotic hands and can even compare to regular grippers when it comes to price. These traits makes them a good choice when considering development of more flexible griping systems to use in industry.

Underactuation in robotic hands leads to some intriguing properties. Underactuated robotic hands cannot always ensure full whole-hand grasping. Distribution of the forces onto the different phalanges is predetermined by the mechanical design of the hand and in some configurations phalanges may not be able to actually exert any force. This uncontrollable force distribution can also lead to unstable grasps: a continuous closing motion of the actuator tending to eject the object [3] as shown on Fig.1.

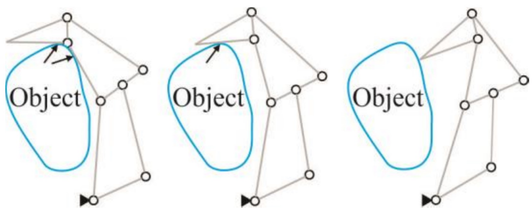

Fig. 1. Unstable grasp of object.

Designing and building underactuated robotic finger that can adapt to any object but can never actually grasp it is futile and to avoid that it is important to do a force analysis of that robotic finger.

In this paper, a new design of the robotic hand, i.e., the CMSysLab Hand, will be presented, focusing to its building block, an uderactuated finger, and within this scope it will be shown how to calculate force that each phalange exerts on object grasped. That information is important in understanding and prevention of above mentioned phenomenon of grasp degeneration and ejection of object.

PhD student Lazar Matijašević is with the Faculty of Mechanical Engineering, University of Belgrade, Kraljice Marije 16, 11120 Belgrade, Serbia (e-mail: lmatijasevic@mas.bg.ac.rs).

Full Professor Petar B. Petrović is with the Faculty of Mechanical Engineering, University of Belgrade, Kraljice Marije 16, 11120 Belgrade, Serbia (e-mail: pbpetrovic@mas.bg.ac.rs).

II. General Analytical Model

In this chapter, a method for obtaining information about force capabilities of robotic n-DoF fingers will be presented. This method is based on approach presented in [4] and [5]. This method will allow one to completely describe the relationship between the input torque of the finger actuator and the contact forces distribution on the phalanges.

For purpose of describing the proposed method, object of grasping will be considered fixed in space and friction will be ignored. Fixing object in space make proposed model predictable and allow for only one finger to be evaluated without the influence of another finger or moving object.

The neglecting friction by itself is very restrictive, but this assumption makes mathematical model relaxed and allows for primary aim of this paper which is to study the capability of the finger, and only finger, to exert contact force on the fixed object. In this stage of our research, our goal is to determine how is actuating torque transmitted through the kinematical chain of the finger and to determine its impact and impact of passive springs on contact force that is exerted on object. Obviously, above mentioned friction properties of contact between object and finger, as well as friction in joints of the finger have tremendous impact on grasping stability, and it will be part of second stage of our research. Friction properties of system are highly unpredictable and including those in this stage of research brings high level of uncertainty to the mathematical model. The significance of such model is questionable without proper experimental results and therefore it will be done with experimental setup that is in finishing stages of design.

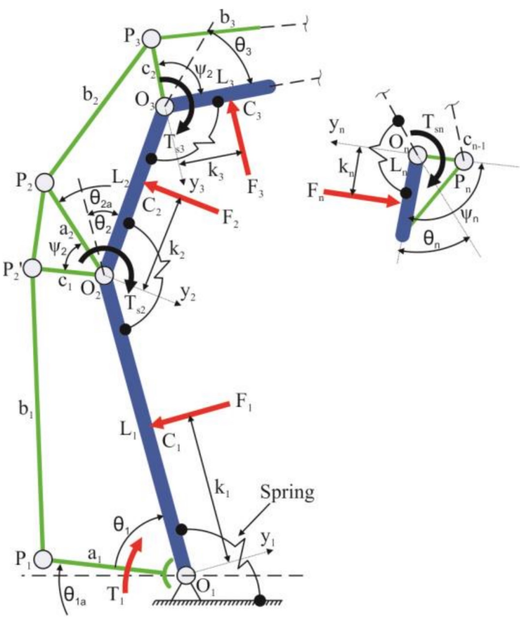

Fig. 2. Representation of n-DoF finger.

An underactuated robotic finger with n phalanges is illustrated in Fig. 2. The input torque from actuator is applied to the first joint of the finger, and it is transmitted to the phalanges through four-bar linkages (FBL).

Adding the springs to the joints results with fully adaptive finger with compliant joints. Passive elements are used to cinematically constrain the finger, and to ensure that finger will adapt to the shape of object being grasped.

The following parameters are presented on Fig. 2:

- L_i - the length of the i^{th} phalanx,
- a_i - the length of the first driving bar of the i^{th} FBL,
- b_i - the length of the i^{th} underactuated bar,
- c_i - the length of the second driving bar of the i^{th} FBL,
- θ_i - the rotating angle of the i^{th} phalanx,
- ψ_i - the angle between O_iP_i' and O_iP_i,
- T_1 - the torque of the actuator at the first joint,
- T_{si} - the spring torque of the i^{th} joint,
- F_i - the contact force of the i^{th} phalanx,
- k_i - position of contact point on the i^{th} phalanx.

In order to determine the distributions of the contact forces that depend on the contact point location and the joint torques inserted by springs, it is necessary to perform a quasi-static modeling of the finger. Equating the input and the output virtual powers of the finger, it yields:

$$T^T \omega_a = F^T v \tag{1}$$

where T represents the input torque vector from the actuator and springs, ω_a is the corresponding velocity vector, F is the contact force vector, and v is the projected velocity vector of the contact points:

$$T = \begin{bmatrix} T_1 \\ T_{s2} = -K_2\Delta\theta_2 \\ T_{s3} = -K_3\Delta\theta_3 \\ \dots \\ T_{sn} = -K_n\Delta\theta_n \end{bmatrix},\ \omega_n = \begin{bmatrix} \dot\theta_{1a} \\ \dot\theta_{2a} \\ \dot\theta_{3a} \\ \dots \\ \dot\theta_n \end{bmatrix},\ F = \begin{bmatrix} F_1 \\ F_2 \\ F_3 \\ \dots \\ F_n \end{bmatrix},\ v = \begin{bmatrix} v_{yc1} \\ v_{yc2} \\ v_{yc3} \\ \dots \\ v_{ycn} \end{bmatrix}, \tag{2}$$

where K_i is the stiffness of the torsional spring in joint O_i, and $\Delta\theta$ is the displacement between the current and initial angles of the joint O_i

Projected velocities can be expressed as a product of a Jacobian matrix J_T and the derivative vector of the phalanx joint coordinates, $\theta = [\theta_1, \theta_2, \theta_3, \dots, \theta_n]^T$:

$$v = J_T \dot\theta . \tag{3}$$

The Jacobian matrix J_T, of the projected velocities, can be obtained in a lower triangular form:

$$J_T = \begin{bmatrix} k_1 & 0 & 0 & \dots & 0 \\ \alpha_{12} & k_2 & 0 & \dots & 0 \\ \alpha_{13} & \alpha_{23} & k_3 & \dots & 0 \\ \dots & \dots & \dots & \dots & \dots \\ \alpha_{1n} & \alpha_{2n} & \alpha_{3n} & \dots & k_n \end{bmatrix};\ \alpha_{ii} = k_i . \tag{4}$$

Matrix member α_{ij} can be calculated:

$$\alpha_{ij} = k_j + \sum_{k=i}^{j-1} L_k \cos\left(\sum_{m=k+1}^{j} \theta_m\right);\ i < j . \tag{5}$$

By using differential calculus, it is possible to relate the vector to the derivatives of the phalanx joint coordinates defined previously with an actuation Jacobian matrix J_a:

$$\dot\theta = J_a \omega_a . \tag{6}$$

In case of underactuated finger model, the four-bar linkage mechanism is used to transmit the actuator torque to each phalanx.

Principle of transmission provides the angular velocity ratio of four-bar linkage that is known as Kennedy's Theorem [6], which states that the three instantaneous centers of rotation shared by three rigid bodies in relative planar motion to another (whether or not connected) all lie on the same straight line.

Considering i^{th} four-bar linkage $O_iP_iP'_{i+1}O_{i+1}$:

$$\dot{\theta}_i = \dot{\theta}_{ia} + \dot{\theta}_{i+1a}\frac{c_i\left(L_i\sin\left(\theta_{i+1a}-\psi_{i+1}\right)-a_i\sin\left(\theta_i-\theta_{ia}+\theta_{i+1a}-\psi_{i+1}\right)\right)}{a_i\left(L_i\sin\left(\theta_i-\theta_{ia}\right)+c_i\sin\left(\theta_i-\theta_{ia}+\theta_{i+1a}-\psi_{i+1}\right)\right)}.$$

Considering last four-bar linkage $O_{n-1}P_{n-1}P_nO'_n$:

$$\dot{\theta}_{n-1} = \dot{\theta}_{n-1a} + \dot{\theta}_n\frac{c_{n-1}\left(L_{n-1}\sin\left(\theta_n-\psi_n\right)-a_{n-1}\sin\left(\theta_{n-1}-\theta_{n-1a}+\theta_n-\psi_n\right)\right)}{a_{n-1}\left(L_{n-1}\sin\left(\theta_{n-1}-\theta_{n-1a}\right)+c_{n-1}\sin\left(\theta_{n-1}-\theta_{n-1a}+\theta_n-\psi_n\right)\right)}.$$

Equation (7) is obtained by substituting equations for $\dot{\theta}_i$ and $\dot{\theta}_{n-1}$ into (6).

$$\begin{bmatrix}\dot{\theta}_1\\ \dot{\theta}_2\\ \dot{\theta}_3\\ \cdots\\ \dot{\theta}_n\end{bmatrix} = \begin{bmatrix}1 & X_1 & 0 & \cdots & 0\\ 0 & 1 & X_2 & \cdots & 0\\ \cdots & \cdots & \cdots & \cdots & \cdots\\ 0 & 0 & 0 & \cdots & X_{n-1}\\ 0 & 0 & 0 & \cdots & 1\end{bmatrix}\begin{bmatrix}\dot{\theta}_{1a}\\ \dot{\theta}_{2a}\\ \dot{\theta}_{3a}\\ \cdots\\ \dot{\theta}_{na}\end{bmatrix}, \qquad (7)$$

where

$$X_i = \frac{c_i\left(L_i\sin\left(\theta_{i+1a}-\psi_{i+1}\right)-a_i\sin\left(\theta_i-\theta_{ia}+\theta_{i+1a}-\psi_{i+1}\right)\right)}{a_i\left(L_i\sin\left(\theta_i-\theta_{ia}\right)+c_i\sin\left(\theta_i-\theta_{ia}+\theta_{i+1a}-\psi_{i+1}\right)\right)}, \qquad (8)$$

$$X_{n-1} = \frac{c_{n-1}\left(L_{n-1}\sin\left(\theta_n-\psi_n\right)-a_{n-1}\sin\left(\theta_{n-1}-\theta_{n-1a}+\theta_n-\psi_n\right)\right)}{a_{n-1}\left(L_{n-1}\sin\left(\theta_{n-1}-\theta_{n-1a}\right)+c_{n-1}\sin\left(\theta_{n-1}-\theta_{n-1a}+\theta_n-\psi_n\right)\right)}. \qquad (9)$$

Function X_i is function that describes the transmition of actuator torque to the i^{th} phalanx.

Equation (10) that provides a practical relationship between the actuator torques and contact forces is derived from (1), (3) and (6):

$$F = J_T^{-T}J_a^{-T}T \qquad (10)$$

This equation is only valid in case when $k_1k_2k_3\ldots k_n \neq 0$, which is the condition of singularity for matrix J_T. Matrix J_a cannot be singular, but, the finger may perform contact with the object in case that number of phalanges in contact with object is fewer than n. This assumption results in a singularity of the matrix J_T, so that (10) is not applicable.

III. Kinetostatic Force Distribution Model

In order for a less-than-n phalanx grasp to be stable, every phalanx in contact with the object should have a strictly positive corresponding force. In grasping process, the contact appear not only with all phalanges, but also with fewer than n phalanges.

The corresponding generated forces for phalanges which are not in contact with the object should be zero, because that forces can also be seen as the external forces needed to counter the actuation torque. However, calculation of contact forces in case of fewer-than-n phalanges touching by object by using Equation (10) can be a problem because of the singularity of the matrix J_T.

This problem can be solved by proposing a general method to determine the distributions of contact forces in all cases of gripper behaviors in object grasping. In order to do that, it is assumed that the stability of the grasp must be satisfied in all cases.

From Equations (10) it is obtained:

$$J_T^TF = J_a^{-T}T, \qquad (11)$$

where the component $J_a^{-T}T$ on the right side is the torque vector $\tau = [\tau_1, \tau_2, \ldots, \tau_n]^T$ at all joints of the finger relating to the actuator, spring torques and functions of torque transmission between actuator and phalanges, which is described by following equation:

$$\begin{bmatrix}\tau_1\\ \tau_2\\ \tau_3\\ \cdots\\ \tau_n\end{bmatrix} = J_a^{-T}T = \begin{bmatrix}1 & X_1 & 0 & \cdots & 0\\ 0 & 1 & X_2 & \cdots & 0\\ \cdots & \cdots & \cdots & \cdots & \cdots\\ 0 & 0 & 0 & \cdots & X_{n-1}\\ 0 & 0 & 0 & \cdots & 1\end{bmatrix}^{-T}\begin{bmatrix}T_1\\ T_{s2}\\ T_{s3}\\ \cdots\\ T_{sn}\end{bmatrix} \qquad (12a)$$

which leads to:

$$\begin{bmatrix}\tau_1\\ \tau_2\\ \tau_3\\ \cdots\\ \tau_n\end{bmatrix} = \begin{bmatrix}T_1\\ T_{s2}-X_1T_1\\ T_{s3}-X_2T_{s2}+X_1X_2T_1\\ \cdots\\ T_{sn}+\sum_{j=1}^{n-1}\left[\left(-1\right)^{n-j}\prod_{i=j}^{n-1}X_iT_{si}\right]\end{bmatrix}, T_{s1}\equiv T_1. \qquad (12)$$

The left part of (11) can be expressed as:

$$J_T^TF = \begin{bmatrix}k_1 & 0 & 0 & \cdots & 0\\ \alpha_{12} & k_2 & 0 & \cdots & 0\\ \alpha_{13} & \alpha_{23} & k_3 & \cdots & 0\\ \cdots & \cdots & \cdots & \cdots & \cdots\\ \alpha_{1n} & \alpha_{2n} & \alpha_{3n} & \cdots & k_n\end{bmatrix}^T\begin{bmatrix}F_1\\ F_2\\ F_3\\ \cdots\\ F_n\end{bmatrix}. \qquad (13)$$

By substituting Equations (12) and (13) in (11), it follows:

$$\begin{bmatrix}\tau_1\\ \tau_2\\ \tau_3\\ \cdots\\ \tau_n\end{bmatrix} = \begin{bmatrix}k_1 & 0 & 0 & \cdots & 0\\ \alpha_{12} & k_2 & 0 & \cdots & 0\\ \alpha_{13} & \alpha_{23} & k_3 & \cdots & 0\\ \cdots & \cdots & \cdots & \cdots & \cdots\\ \alpha_{1n} & \alpha_{2n} & \alpha_{3n} & \cdots & k_n\end{bmatrix}^T\begin{bmatrix}F_1\\ F_2\\ F_3\\ \cdots\\ F_n\end{bmatrix}. \qquad (14)$$

This equation shows that the torque τ_i at the i^{th} joint of the finger is calculated with respect to the contact forces vector F and parameters α_{ij}, as shown in following equation:

$$\sum_{j=i}^{n}\alpha_{ij}F_j = \tau_i,\ \ \alpha_{ii} = k_i\ . \qquad (15)$$

In case when number of phalanges in contact with object is fewer than n (e.g., when the i^{th} phalanx is not touching the object), the parameters α_{ij} in (15) are not relevant and F_i is zero. This means that (15) does not meet this condition, so it is not considered when computing the torque τ_i in case when the i^{th} phalanx is not touching the object. In order to calculate the contact forces vector F in (14), except for F_i, the following process must be used:

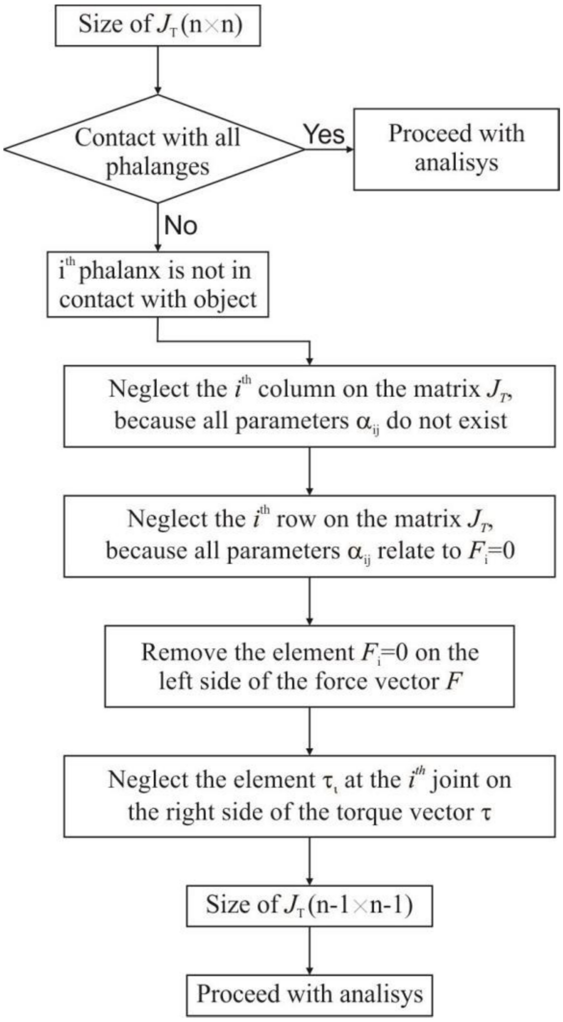

Fig. 3. Algorithm for calculating force parameters in case when not all phalanges are in contact with object.

After neglecting the i^{th} column and i^{th} row, dimension of the matrix J_T is reduced by $n-1 \times n-1$, while it is guaranteed that matrix J_T will not be singular. Consequently, Equation (14) can be used in order to calculate the contact forces, except for force F_i on the i^{th} phalanx. The same process is also used in case when more than one phalanx is not in contact with the object.

IV. CMSysLab Hand finger design

Aim of this research is to develop multifingered underactuated hand for use in industry setting for tasks of extremely diversified robotic assembly and enable ubiquitous use in industry, in particular SME compatibility. For this purpose we have entered in development of the underactuated robotic finger that uses sets of linkages to transmit torque from actuator to phalanges. CMSysLab Hand finger is designed in such a manner that it allows easy installation of various sensors and building various configurations of the multifingered hands, including reconfigurable hands, making it optimal building block for various research purposes. Underactuated robotic finger design for CMSysLab Hand has three phalanges and therefore 3-DoF.

Parameters of finger for CMSysLab robotic hand are based on actual proportions of finger of human hand. The set of parameters presented in Table 1 is taking into account the mechanical joint limits, which are key elements in the design of underactuated fingers, when considering stability issues, because they limit the shape adaptation to reasonable configurations.

TABLE I
Parameters of CMSysLab underactuated finger

a_1 [mm]	30	a_2 [mm]	23
b_1 [mm]	60.5	b_2 [mm]	37
c_1 [mm]	15	c_2 [mm]	14
L_1 [mm]	64.5	ψ_2 [°]	52
L_2 [mm]	37.5	ψ_3 [°]	90
L_3 [mm]	34.5		

Geometric and contact force parameters of underactuated 3-DoF finger are described in Fig. 4.

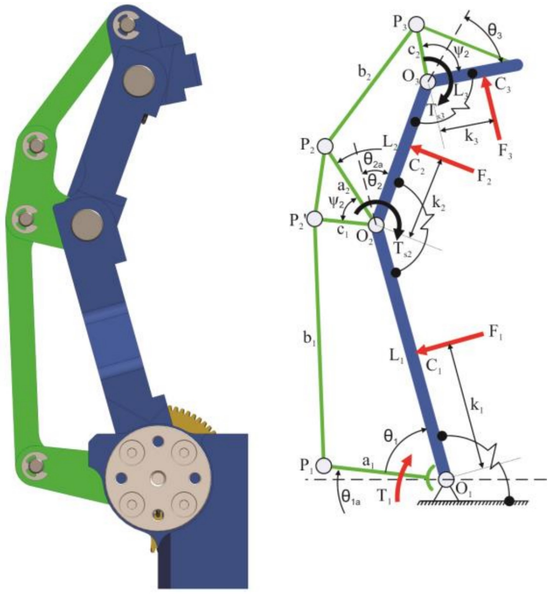

Fig. 4. Geometric and force parameters of underactuated 3-DoF finger.

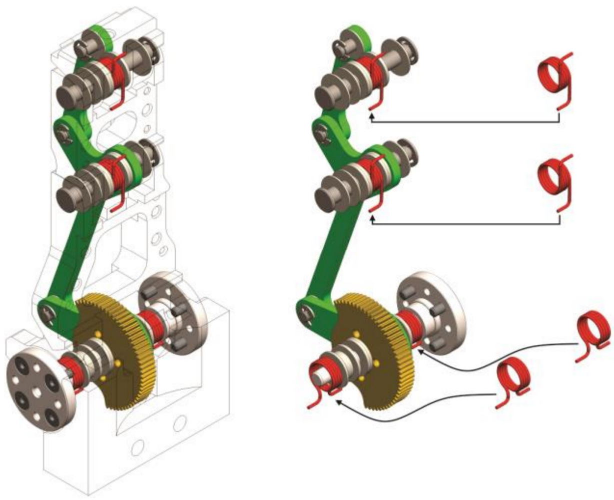

Fig. 5. Mechanical structure of underactuated 3-DoF finger.

The behavior of the finger is mostly determined by its geometry. Depending on the geometric parameters of the mechanism, it is possible to obtain the final stability of the grasp. In structure of the finger, shown on Fig. 5, mechanical limit is used, which allows a pre-loading of the spring , shown with red color, to prevent any undesirable motion of the medial and distal phalanges, due to its own weight and/or inertial effects, as well to prevent hyperflexion of the finger. In Fig. 6 workspace as well as pre-forming stages of such finger are shown.

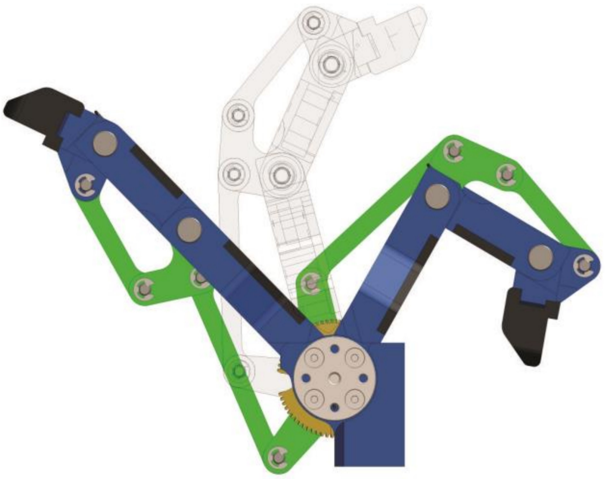

Fig. 6. Workspace of underactuated 3-DoF finger.

V. CONTACT FORCE ANALYSIS

In case of the underactuated finger with 3-DoF, (10) holds if and only if $k_1k_2k_3 \neq 0$, which represents the condition of singularity for the matrix J_T, as shown in Fig. 5. There are however other cases, where finger can contact the object when one or two phalanges of the finger are not touching the object, which is shown in Fig. 7, 8,9 and 10.

In order to calculate the contact forces F_1, F_2 and F_3 on the grasping object, it is necessary to separate four cases of possible behaviors between the finger and the object during grasping process.

Case 1: All three phalanges of the finger are in contact with the object, so $k_1k_2k_3 \neq 0$, as shown in Fig. 7.

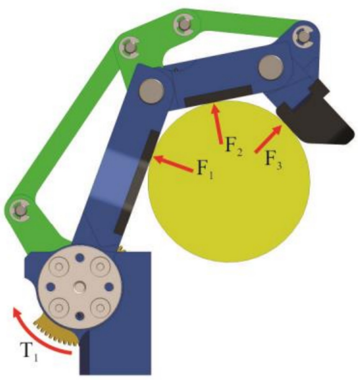

Fig. 7. Representation of 3-DoF robotic finger in case were all phalanges are in contact with grasped object.

The relationship between the actuator torques and contact forces can be derived from (14):

$$\begin{bmatrix} k_1 & k_2+L_1C_2 & k_3+L_1C_{23}+L_2C_3 \\ 0 & k_2 & k_3+L_2C_3 \\ 0 & 0 & k_3 \end{bmatrix}\begin{bmatrix} F_1 \\ F_2 \\ F_3 \end{bmatrix} = \begin{bmatrix} T_1 \\ T_{s2}-X_1T_1 \\ T_{s3}-X_2T_{s2}+X_1X_2T_1 \end{bmatrix}. \quad (16)$$

From previous equation, the three contact forces F_1, F_2 and F_3 can be computed by using Equations (17), (18) and (19), respectively:

$$F_1 = \frac{T_1}{k_1} - \frac{(k_2+L_1C_2)(T_{s2}-X_1T_1)}{k_1k_2} - \frac{(k_3+L_1C_{23}+L_2C_3)(T_{s3}-X_2T_{s2}+X_1X_2T_1)}{k_1k_3} + \frac{(k_2+L_1C_2)(k_3+L_2C_3)(T_{s3}-X_2T_{s2}+X_1X_2T_1)}{k_1k_2k_3} \quad (17)$$

$$F_2 = \frac{T_{s2}-X_1T_1}{k_2} - \frac{(k_3+L_2C_3)(T_{s3}-X_2T_{s2}+X_1X_2T_1)}{k_2k_3} \quad (18)$$

$$F_3 = \frac{T_{s3}-X_2T_{s2}+X_1X_2T_1}{k_3} \quad (19)$$

Case 2: The proximal and distal phalanges are in contact with the object, which means that parameter k_2 does not exist, while force F_2 is zero, as illustrated in Fig. 8.

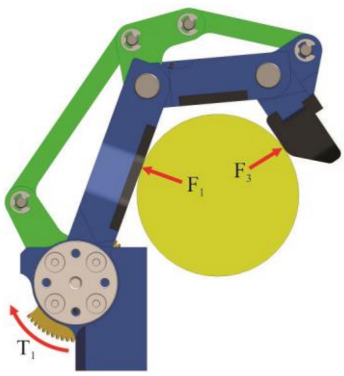

Fig. 8. Representation of 3-DoF robotic finger in case were proximal and distal phalanges are in contact with grasped object.

In Equation (16), the second column and second row in the matrix J_T relating to the medial phalanx are removed, as well as the force F_2 and the torque $\tau_2 = T_{s2} - X_1T_1$ in the vectors F and τ. After removal of aforementioned elements, (16) obtains the following form:

$$\begin{bmatrix} k_1 & k_3+L_1C_{23}+L_2C_3 \\ 0 & k_3 \end{bmatrix}\begin{bmatrix} F_1 \\ F_3 \end{bmatrix} = \begin{bmatrix} T_1 \\ T_{s3}-X_2T_{s2}+X_1X_2T_1 \end{bmatrix}, \quad (20)$$

where forces F_1 and F_3 are calculated using (21) and (19), respectively:

$$F_1 = \frac{T_1}{k_1} - \frac{(k_3+L_1C_{23}+L_2C_3)(T_{s3}-X_2T_{s2}+X_1X_2T_1)}{k_1k_3}. \quad (21)$$

Case 3: The medial and distal phalanges are in contact with the object, which means that parameter k_1 does not exist, while force F_1 is zero, as illustrated in Fig. 9.

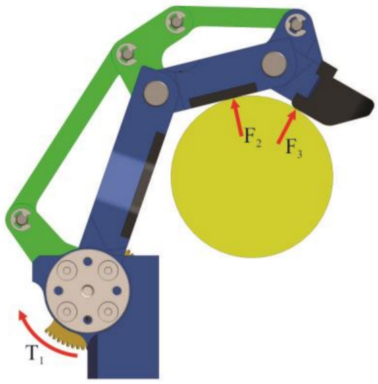

Fig. 9. Representation of 3-DoF robotic finger in case were medial and distal phalanges are in contact with grasped object.

In Equation (16), the first column and first row in the matrix J_T relating to the proximal phalanx are removed. Also, the elements F_1 and τ_1 in the force vector F and torque vector τ are removed. Then (16) becomes:

$$\begin{bmatrix} k_2 & k_3 + L_2 C_3 \\ 0 & k_3 \end{bmatrix} \begin{bmatrix} F_2 \\ F_3 \end{bmatrix} = \begin{bmatrix} T_{s2} - X_1 T_1 \\ T_{s3} - X_2 T_{s2} + X_1 X_2 T_1 \end{bmatrix}, \quad (22)$$

where F_2 and F_3 are calculated by using (18) and (19), respectively.

Case 4: Only the distal phalanx is in contact with the object, which means that parameters k_1 and k_2 do not exist, while elements F_1 and F_2 of force vector F are zero, as illustrated in Fig. 10.

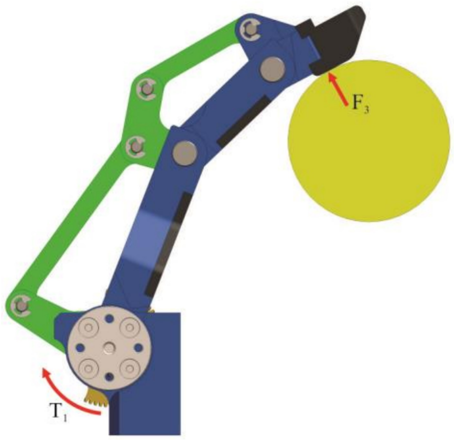

Fig. 10. Representation of 3-DoF robotic finger in case were only distal phalanx is in contact with grasped object.

In Equation (16), the first and second column and row in the matrix J_T relating to the proximal and medial phalanges are removed, as well as the elements F_1 and F_2 of the force vector F, and element τ_2 of the torque vector τ. Then, Equation (16) becomes:

$$k_3 F_3 = T_{s3} - X_2 T_{s2} + X_1 X_2 T_1, \quad (23)$$

where F_3 is calculated by using Equation (19).

VI. Conclusion

In this paper, a method for obtaining information of the force acting upon phalanges was presented. This kind of force analysis is important so that researchers and designers of underactuated robotic hands can design proper underactuated finger that has stable grasp of object. These hands have to be robust enough and to have stable grasp if they were to be used in industry setting.

As part of future research this proposed mathematical model for analysis of force distribution on phalanges is going to be supplemented with actual experimental results from experiments with first two finger underactuated CMSysLab Hand.

Future work on CMSysLab Hand will also include simulation of this hand in various softwares and authentication of results through experiments. Design of CMSysLab Hand allows the hand to be equipped with different sensory systems so that experiments can be done.

Future research also must include optimization of four-bar linkages and calculation and optimization of springs that are used to counter inertial effects due to phalanges own weight and friction.

Acknowledgment

This research work is supported by the Serbian Ministry for Education, Science and Technology Development through the projects titled 'Smart Robotics for Customized Manufacturing', grant No.: TR35007, and 'Development and Experiments of Mobile Collaborative Robot With Dual-Arm', grant No.: 401-00-00589/2018-09, which is jointly realized by Anhui University of Technology, Ma'anshan, Anhui, and Tsinghua University, Beijing, from one side, and Institute Mihajlo Pupin – Belgrade (IMP), Faculty of Mechanical Engineering, University of Belgrade (MFB), and Faculty of technical sciences of Novi Sad, University of Novi Sad (FTN), from the other side, supported by a cluster of industrial partners from both sides, as a bilateral scientific project of high national relevance with the Public Republic of China.

References

[1] Bullock, M., Ma, R., Dollar, A.:"A Hand-Centric Classification of Human and Robot Dexterous Manipulation", *IEEE Transactions on Haptics*, vol. 6, pp. 129-144, April-June 2013.

[2] Paul Tuffield, Hugo Elias "The Shadow robot mimics human actions", *Industrial Robot: An International Journal*, vol. 30 Issue: 1, pp.56-60, 2003.

[3] L. Birglen ; C.M. Gosselin "Kinetostatic Analysis of Underactuated Fingers", *IEEE Transactions on Robotics and Automation*, vol. 20 Issue: 1, pp.211 -221, april 2004

[4] Birglen, Lionel, Laliberté, Thierry, Gosselin, Clément M. "Kinetostatic Analysis of Underactuated Fingers" in Underactuated Robotic Hands, Springer-Verlag Berlin Heidelberg, 2008, ch. 3, pp. 33-60.

[5] Xuan Vinh Ha, Cheolkeun Ha and Dang Khoa Nguyen: "A General Contact Force Analysis of an Under-actuated Finger in Robot Hand Grasping" *International Journal of Advanced Robotic System,* vol. 13, Issue 1, December 2015.

[6] McCarthy, J. Michael, Soh, Gim Song "Analysis of Planar Linkages" in Geometric Design of Linkages, Springer-Verlag New York, 2011, ch. 2, pp. 15-53.